

An In Silico Approach to Discovering Novel Inhibitors of Human Sirtuin Type 2

Anu J. Tervo,^{*,†,‡} Sergiy Kyrylenko,[§] Päivi Niskanen,[†] Antero Salminen,^{§,||} Jukka Leppänen,[†] Tommi H. Nyrönen,[‡] Tomi Järvinen,[†] and Antti Poso[†]

Department of Pharmaceutical Chemistry and Department of Neuroscience and Neurology, University of Kuopio, P.O. Box 1627, 70211 Kuopio, Finland, CSC—Scientific Computing Ltd., P.O. Box 405, 02101 Espoo, Finland, and Department of Neurology, Kuopio University Hospital, P.O. Box 1777, 70211 Kuopio, Finland

Received January 23, 2004

Type 2 human sirtuin (SIRT2) is a NAD⁺-dependent cytoplasmic protein that is colocalized with HDAC6 on microtubules. SIRT2 has been shown to deacetylate α -tubulin and to control mitotic exit in the cell cycle. To date, some small molecular inhibitors of SIRT2 have been identified; however, more inhibitors are still needed to improve the understanding of SIRT2 biological function and to discover its possible therapeutic indications. In this paper, an in silico identification procedure is described for discovering novel SIRT2 inhibitors. Molecular modeling and virtual screening were utilized to find potential compounds, which were then subjected to experimental tests for their SIRT2 inhibitory activity. Five of the 15 compounds tested in vitro showed inhibitory activity toward SIRT2, yielding a hit ratio of 33% in a micromolar level and thus demonstrating the usefulness of this procedure in finding new bioactive compounds. Two of the five compounds yielded in vitro IC₅₀ values of 56.7 and 74.3 μ M, and these can be considered as novel inhibitors of SIRT2. On the basis of our results, a phenol moiety on the active compound is suggested to be important for SIRT2 inhibitory activity. This phenol group, together with a hydrophobic moiety and hydrogen-bonding features, is suggested to form an active SIRT2 pharmacophore.

Introduction

The silent information regulator Sir2 and Sir2-like proteins (SIRT1–SIRT7, sirtuins) belong to the category of class III histone deacetylases (HDACs).¹ In yeast, this acetyl transfer reaction catalyzed by Sir2 has been shown to be NAD⁺-dependent,^{2,3} forming *O*-acetyl-ADP-ribose and nicotinamide as reaction products.^{4–7} In yeast, Sir2 proteins play a vital role in transcriptional gene silencing at the mating type loci, telomeres and rDNA.^{8–11} Their function has been suggested to be related to the aging process^{12–14} and some cancers,^{15,16} for example.

Human sirtuin type 2 (SIRT2), one of the seven human Sir2 homologues so far identified,^{17,18} is a cytoplasmic protein that is colocalized with HDAC6 on microtubules.¹⁹ SIRT2 has been shown to deacetylate α -tubulin¹⁹ and control mitotic exit within the cell cycle.²⁰ The structure of SIRT2 has been crystallized and solved with a resolution of 1.70 Å.²¹ This protein structure consists of 389 amino acids. It has a catalytic core with two domains and an N-terminal helical extension. The larger domain is a variant of the Rossmann fold²² and is connected by several conserved loops to the smaller domain. A large groove is formed at the interface of these two domains. The smaller domain is composed of a zinc-binding module with a zinc ion tetrahedrally coordinated with four cysteine residues and a helical module consisting of four α -helices. The helical module contains a pocket that is lined with

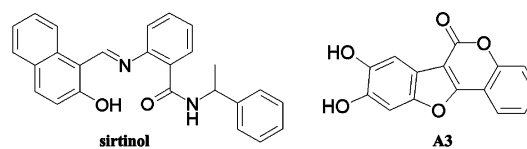


Figure 1. Known inhibitors of SIRT2.

solvent-exposed hydrophobic residues. This pocket intersects the large groove. Its properties suggest that it may recognize portions of the substrate and be a class-specific protein binding site.²¹

To date, several small molecular inhibitors of yeast Sir2p have been identified.^{23,24} Two of them, 2-{{[1-(2-hydroxynaphthalen-1-yl)meth-(*E*)-ylidene]amino}-*N*-(1-phenylethyl)benzamide (sirtinol) and 8,9-dihydroxybenzo-[4,5]furo[3,2-*c*]chromen-6-one (A3) (both presented in Figure 1), show inhibitory activity toward human SIRT2 as well.²⁴ These two inhibitors have reported IC₅₀ values of 38 and 45 μ M against SIRT2, respectively. For further development to progress, it is essential to find novel inhibitors of SIRT2 to improve the understanding of its biological function²⁵ and to discover its possible therapeutic indications. In this paper, an identification procedure for new compounds having SIRT2 inhibitory activity is described. The procedure utilized both molecular modeling and virtual screening, and the resulting identified hit compounds were tested in vitro for their SIRT2 inhibitory activity.

Results

Preparing the Enzyme Structure. The X-ray structure of SIRT2 was preprocessed by molecular dynamics (MD) simulation. The average structure from the last 50 ps of simulation was calculated and energy-mini-

* To whom correspondence should be addressed. Tel: +358-9-4572228. Fax: +358-9-4572302. E-mail: anu.tervo@csc.fi.

[†] Department of Pharmaceutical Chemistry, University of Kuopio.

[‡] CSC—Scientific Computing Ltd.

[§] Department of Neuroscience and Neurology, University of Kuopio.

^{||} Kuopio University Hospital.

Table 1. Amino Acids That Were Considered To Form the Putative SIRT2 Active Site

amino acid	secondary structure ^a
Asp95, Phe96, Arg97, Leu103, Tyr104	L1
Leu107	α 3
Leu112, Pro115, Glu116, Ile118, Phe119	α 4
Tyr123, Phe124	α 5
Phe131, Leu134, Leu138	α 6
Gln167, Asn168, Ile169, Asp170	L2
His187, Gly188, Phe190	L3
Phe235	L4

^a Secondary structure in which the presented amino acids belong (α , α -helix; L, loop region).

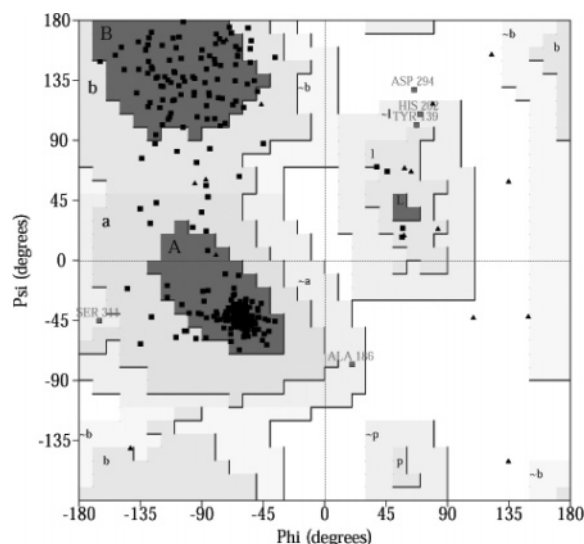


Figure 2. Ramachandran plot of the final SIRT2 structure after the MD simulation. The amino acid located in the disallowed region, Asp294, is not part of the putative SIRT2 active site.

mized and then used as the SIRT2 enzyme structure in the study. A heavy atom root-mean-square deviation (rmsd) value between this final structure and the energy-minimized starting structure of the MD simulation was 3.84 Å. A corresponding rmsd value of 3.56 Å was obtained for the amino acids of the putative SIRT2 active site (Table 1). These values were relatively high, although some fluctuations in rmsd from MD simulation can be accepted. Inspection of the enzyme structure showed that the structural rearrangements of the amino acids were related to different side chain conformations in several cases. These rearrangements resulted in an enlargement of the hydrophobic pocket at the putative binding site. Therefore, it was necessary to carry out a further quality check by evaluating the final SIRT2 structure with the PROCHECK program.²⁶ A total of 98% of all amino acid residues were located in the core or allowed regions of the Ramachandran plot²⁷ (Figure 2). The amino acid residue located in the disallowed region, Asp294, was not part of the putative SIRT2 active site. In general, the quality level of the final structure was similar to that of the original monomer B of 1j8f. PROCHECK results indicated that both structures had an average quality of an X-ray structure solved with a resolution of 1.70 Å. These results suggested that the quality of the final SIRT2 structure was sufficient for further analyses and that the active site of the final SIRT2 structure could be accepted for virtual screening purposes in our study.

Examining the Putative SIRT2 Active Site. The putative SIRT2 active site was examined with the program GRID²⁸ to determine favorable interactions. These results were examined by visualizing the interaction fields with the amino acids of the active site. (See the Supporting Information for the graphical representations of the relevant interaction fields.) From the utilized probes, the tetrahedral cationic NH_2^+ group (NH_2^+) had an interaction energy of -13 kcal/mol near the backbone carbonyl oxygen of Phe119 and near backbone carbonyl oxygens and NH groups of His187, Gly188, and Val233. The phenolic and carboxy hydroxyl group probe (OH) yielded an interaction energy of -11 kcal/mol near the carboxyl group of Asp95 and the amine side chain of Arg97. Interestingly, the water probe resulted in a highly favorable interaction energy of -16 kcal/mol inside the narrow channel, which began at the putative active site near the amino acids Ile169 and Asp170 and continued throughout the length of the entire enzyme. Together with observations from the X-ray structure, these results verify the highly hydrophilic nature of the channel. The water probe resulted in no interactions in the corresponding energy levels for the hydrophobic area of the putative active site. Other examined probes resulted in insignificant interaction energies and thus were given less attention. Hydrophobic DRY and methyl group probes resulted in reasonable interaction energies (-1.5 and -3.5 kcal/mol, respectively), which also provide evidence for the hydrophobic nature of the putative active site.

The known inhibitors sirtinol and A3 were docked at the putative SIRT2 active site to obtain information on their potential binding conformations and to obtain further evidence for GRID interaction calculations. Therefore, all docked conformations of both inhibitors were inspected. As a flexible compound, sirtinol gave several reasonable docked conformations. A representative conformation of the most common docked orientations of sirtinol is presented in Figure 3A. A common feature of all these conformations was the eagerness of the aromatic ring moieties to interact with the hydrophobic portions of the residues Pro115, Phe119, Leu138, Ile169, Phe190, and Ile232. This suggests that receptor hydrophobicity might be important for inhibitor binding. The rigid compound A3 yielded only one effective docked conformation (Figure 3B). In this conformation, the phenolic hydroxyl groups of A3 were able to form hydrogen bonds with the carboxyl group of Asp95. In addition, the phenolic hydroxyl groups were located in the same area as the favorable interaction energy field of the OH probe. This suggests the importance of an interaction between the inhibitor's hydroxyl group and either Asp95 or Arg97.

Virtual Screening Procedure. Two search queries were created for database searching. The queries were based on the properties of the putative SIRT2 active site (hydrophobicity and shape of the cavity) and GRID examinations (favorable interactions of NH_2^+ and OH probes). Docking studies of the known inhibitors additionally confirmed the interaction region of the phenolic hydroxyl group and a favorable interaction with the hydrophobic pocket. Database searching from Maybridge²⁹ returned 66 candidate compounds, of which 44 compounds passed the in silico intestinal absorption

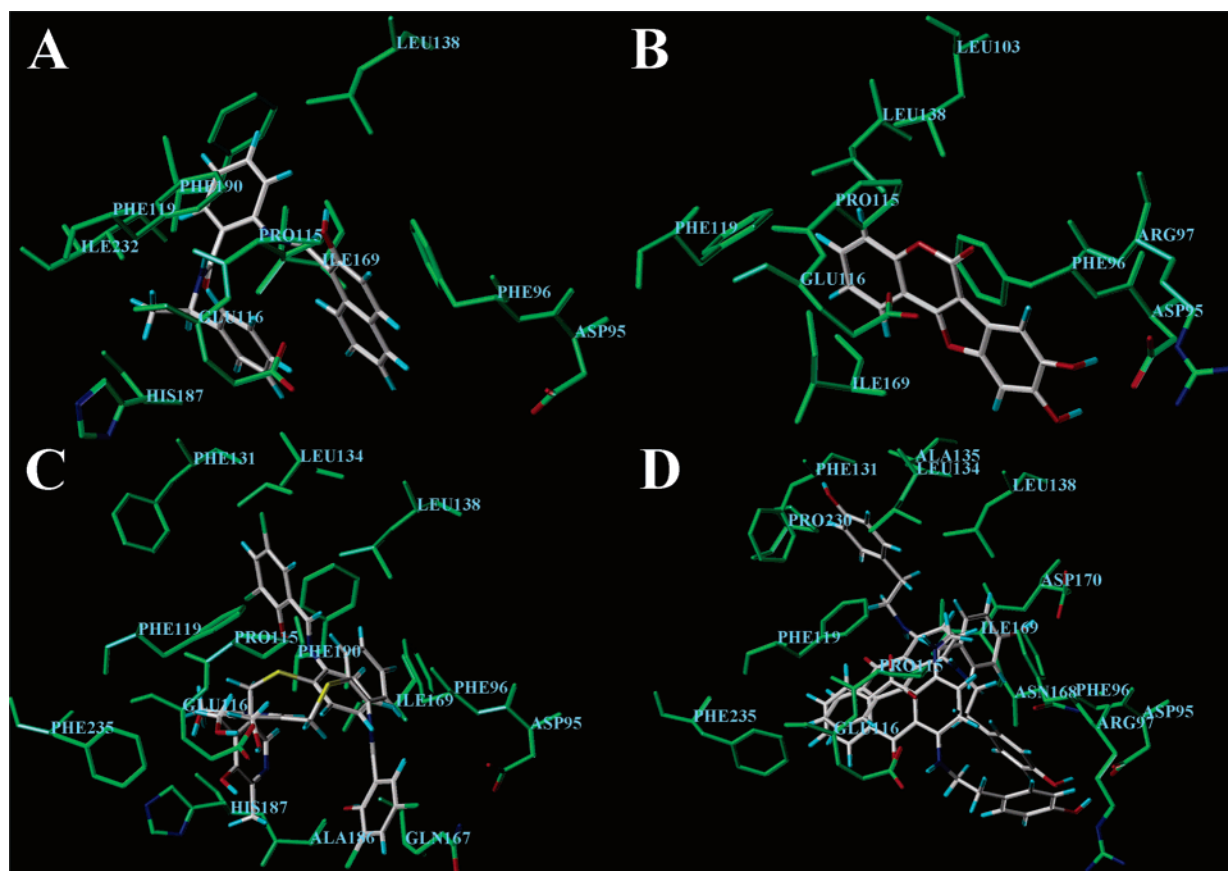


Figure 3. Four docked inhibitors at the putative active site of SIRT2. Amino acids are colored in green, except the heteroatoms of the side chains. The hydrogens of the amino acids are omitted for clarity. (A) Representative docked conformation of sirtinol. (B) Docked conformation of A3. (C) Two representative docked conformations for inhibitor **2**. (D) Two representative docked conformations for inhibitor **5**.

ability filter. These 44 compounds were docked at the putative SIRT2 active site to examine if they fulfilled the requirements presented in the search queries in their docked conformations. Like sirtinol, most compounds readily interacted with the hydrophobic pocket of the active site. However, several compounds were excluded because their docked conformations were inside the hydrophobic pocket, but they failed to fulfill other search requirements; e.g., the ability to sterically block the opening of the narrow channel or to have an OH or SH functional group near Asp95 or Arg97. On the basis of these examinations, 15 compounds were selected for in vitro testing of their SIRT2 inhibitory activity.

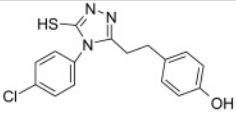
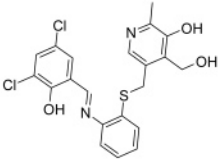
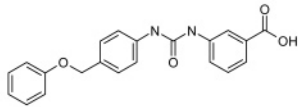
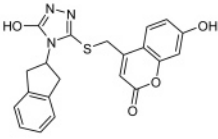
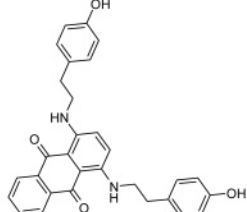
Inhibition of SIRT2. SIRT2 inhibitory activity was tested for 15 compounds. Five of the tested compounds showed inhibitory activity toward SIRT2 (Table 2), yielding an experimental hit ratio of 33%. Compounds **2** and **5** inhibited SIRT2 with an activity level comparable to that of sirtinol (Table 3), yielding IC_{50} values of 74.3 and 56.7 μ M, respectively. In addition, compounds **1**, **3**, and **4** showed a slight inhibition of SIRT2 (Table 2). The rest of the compounds did not show SIRT2 inhibition at the micromolar level, and these were not considered to be active (see the Supporting Information for the structures). On the basis of the docking results for the 15 tested compounds, plus sirtinol and A3, it was impossible to separate active inhibitors from inactive compounds when using the interaction geometries or the GOLD rank scores for the docked conformations as a separation criteria.

Discussion

Sirt2 proteins are NAD^+ -dependent histone deacetylase enzymes.^{1–3} However, two of the seven mammalian SIRT2s that have been characterized so far can also deacetylate nonhistone proteins; i.e., the p53 protein by SIRT1³⁰ and α -tubulin by SIRT2.¹⁹ Interestingly, acetylated α -tubulin is a specific substrate for SIRT2, as other SIRT2s were unable to deacetylate α -tubulin.¹⁹ The acetylation of α -tubulin increases the microtubular stability, which is important in neuronal axon and dendrite pathology, for example. A strong reduction in tubulin acetylation has been observed in neurons containing Alzheimer's τ tangles.³¹ Furthermore, SIRT2 controls the mitotic exit of the cell cycle,²⁰ probably by regulating spindle microtubules. In addition to SIRT2, HDAC6 can also deacetylate Lys40 of α -tubulin in microtubules.³² However, SIRT2 is a NAD^+ -dependent enzyme, which means that energy deficiency due to hypoxia or ischemia may activate SIRT2 and increase microtubular instability. Hence, SIRT2 seems to provide a novel target for drug development for several indications.

We have described an identification method for new and potent inhibitors of SIRT2. Different molecular modeling methods were utilized in studying the SIRT2 enzyme structure. The structure and favorable interactions in the putative SIRT2 active site were used as a starting point for searches performed in the Maybridge database.

Table 2. Structures of the Compounds Showing SIRT2 Inhibitory Activity

Compd Structure	Code ^a	IC ₅₀ ^b
	BTB01093	> 300 μM
	CD04097	74.3 μM
	HTS04977	> 300 μM
	HTS08006	> 300 μM
	JFD00244	56.7 μM

^a Compound code number in the Maybridge database. ^b Measured inhibitory activity expressed as the IC₅₀ of SIRT2.

Table 3. Inhibition of SIRT2 Activity by Sirtinol, Nicotinamide, and the Hit Compounds **2** and **5**

inhibitor	IC ₅₀ (μM) of SIRT2 ^a	
	average	stdev
sirtinol	45.1	1.6
NA ^b	100.5	14.1
2	74.3	1.5
5	56.7	4.2

^a Average and standard deviation (stdev) values were obtained from the IC₅₀ determinations performed in triplicate. ^b Nicotinamide.

From the search results, 15 compounds were chosen for in vitro testing of their SIRT2 inhibitory activity. Five of these compounds showed SIRT2 inhibitory activity, yielding an experimental hit ratio of 33%. This high percentage undoubtedly demonstrates the usefulness of computer-based methods as another tool in finding new bioactive compounds for a target protein. The overall ability of the tested compounds to inhibit SIRT2 is considered to be effective, as two of the most potent inhibitors, **2** and **5**, inhibited SIRT2 with an activity level comparable to that of sirtinol (Table 3). It should be noted that we were able to utilize the experimentally solved high-resolution X-ray structure of SIRT2²¹ in our research, which offered a valuable

starting point for examining properties of the active site and allowed us to base molecular modeling studies on experimental information.

The structures of the five identified compounds give suggestions for properties that are important to SIRT2 inhibitory activity. All compounds contain at least one hydroxyl group. This functional group is a part of either the phenol or benzoic acid moiety in these five compounds, whereas in the 10 inactive compounds the hydroxyl group can also be present as a part of the carboxylic acid or as an alcohol. Moreover, compounds **2** and **5** contain two phenolic moieties in their structures. This result indicates the importance of an acidic hydroxyl group, preferably as a part of a phenolic moiety. Grozinger et al.²⁴ already proposed the 2-hydroxy-1-naphthaldehyde moiety as being primarily responsible of the inhibitory activity of sirtinol, and this suggestion is consistent with our findings. According to our results, naphthaldehyde can be reduced to a phenolic moiety without the loss of its inhibitory activity. On the basis of the molecular structures of sirtinol, A3, 2-hydroxy-1-naphthaldehyde, and our active hit compounds, it seems beneficial if an acidic hydroxyl group is capable of acting as a hydrogen-bond donor. There was no obvious correlation between molecular weight or the amount of acidic hydroxyl groups with activity, as several of the tested compounds had two phenolic moieties without showing any detectable inhibition of SIRT2. The active compounds contain more than one hydrogen-bond donor and acceptor, as well as a hydrophobic moiety in their structures. Thus, a combination of these properties with one or more acidic hydroxyls, preferably phenols, may form a SIRT2 pharmacophore.

The docked conformations of the novel inhibitors **2** and **5** were also examined within the putative SIRT2 active site. Both inhibitors provided several docked conformations, and the two most commonly occurring orientations for both inhibitors are discussed (Figure 3C and 3D for inhibitors **2** and **5**, respectively). For inhibitor **2**, these two orientations were considerably different. A hydrogen bonding possibility to the backbone carbonyl oxygen of Gln167 was observed for the hydroxyl group of the 3,5-dichloro-2-hydroxyphenyl ring for one of these docked conformations. In the other conformation, this ring moiety was oriented toward the hydrophobic pocket near Phe119, Phe131, Leu134, Leu138, and Phe190. In both of the docked conformations for inhibitor **2**, the aromatic ring had hydrophobic interactions with Phe96 and Ile169 and the 4-hydroxymethyl-2-methylpyridin-3-ol ring was located near Pro115, Glu116, and Phe235. The two docked orientations of inhibitor **5** had the anthraquinone moiety docked deeper into this area, more toward the aromatic rings of Phe119 and Phe235. Both docked orientations of inhibitor **5** also had one phenol ring near Asp95 and Arg97, enabling hydrogen bonding for the phenolic hydroxyl group with either the carboxyl group of Asp95 or the side chain amine group of Arg97. The amine group in one of the docked conformations could also form a hydrogen bond with the carboxyl group of Glu116. The other phenolic ring of inhibitor **5** was, however, docked differently in these two orientations. In one docked conformation, this phenolic ring was pointing toward the narrow channel present at the putative active site. In this position, the phenolic

hydroxyl group could make hydrogen bonds to the backbone NH group of Ile169 or to the carboxyl group of Asp170. Hydrophobic parts of Phe96, Leu138, and Ile169 were surrounding the phenol ring. In the other docked conformation, the phenolic ring was docked deeper into the hydrophobic pocket close to the hydrophobic side chains of Phe131, Leu134, Leu138, and Pro230.

On the basis of these docking results, a common interaction mode for sirtinol, A3, and the inhibitors **2** and **5** with amino acids of the putative SIRT2 active site could not be obtained. Hydrophobic moieties of these inhibitors tend to interact with the hydrophobic pocket of the active site. Thus, amino acids commonly present in hydrophobic interactions, like Phe96, Phe131, Leu134, Leu138, and Phe190, could be observed in close proximity for the majority of the docked inhibitors. Hydrogen bonding between the inhibitors and the amino acids was not observed to have a primary role in inhibitor binding. This observation is in line with the highly hydrophobic nature of the putative SIRT2 active site. A common favorable interaction was observed for the phenolic moiety of A3, **2**, and **5** near Asp95 and Arg97. However, the 2-hydroxy-1-naphthaldehyde moiety of sirtinol did not achieve a similar docked orientation in this area. Therefore, these docking results suggest that some common pharmacophoric elements for the inhibitors could be identified, but inhibitors may still obtain different binding orientations at the active site.

Experimental Section

Molecular Modeling. Unless noted otherwise, molecular modeling was performed using Sybyl versions 6.8 and 6.8.1.³³

Preparing the Enzyme Structure. The human SIRT2 X-ray structure was retrieved from the Protein Data Bank³⁴ (PDB code 1j8f²¹). The structural data was obtained from a crystallized 323-amino acid fragment of SIRT2, which possessed histone deacetylase activity comparable to full-length SIRT2.²¹ SIRT2 is a monomer in solution,²¹ and therefore only the monomer (B) was chosen from the trimeric SIRT2 structure of 1j8f for this research. Monomer B was selected as it showed the least amount of defects in structure when examined with the Protein Health program in Quanta 2000.³⁵ The 3D structure of amino acids Ser46–Glu56 from the N-terminal helical extension was not determined in 1j8f; therefore, a short fragment consisting of amino acids Gly34–Phe45 was removed from the overall structure.

The hydrophobic pocket suggested as a class-specific binding site of SIRT2 by Finnin et al.²¹ was of particular interest in this study. The amino acids forming this pocket belonged to three α -helices of the helical module ($\alpha 3$ –6) or to the conserved loops between the two domains (L1 and L4). This hydrophobic pocket intersects the large groove between the two domains, thus being a part of a wider cavity on the enzyme surface. Therefore, amino acids in this large groove that were close to the hydrophobic pockets were also considered as a part of the putative binding site in the study. These amino acids belonged to the conserved loops L1–L3 and L5.²¹ Overall, the putative SIRT2 active site was considered to consist of the amino acids presented in Table 1.

1j8f was crystallized in an uncomplexed form. The X-ray structure might also contain residual energetic tensions after crystallization. Thus, an energetically favorable conformation of the putative binding site was investigated by carrying out an energy minimization of the crystallized enzyme structure with the steepest descent method, followed by a standard MD simulation with the program GROMACS 3.0.1.³⁶ A MD simulation of 400 ps was performed in an aqueous box using the Gromos-96 force field,^{37,38} the SPC water model,³⁹ and a

time step of 2.0 fs. The enzyme structure, water molecules, and the zinc ion were separately coupled to a heat bath at a temperature of 300 K with the Berendsen algorithm⁴⁰ as a thermostat, using a coupling constant of 0.1 ps. Pressure was coupled with the Berendsen algorithm⁴⁰ as a barostat, using a time constant of 1.0 ps. In the zinc-binding module of the smaller domain, the distances between the zinc ion and sulfur atoms of the cysteine residues (Cys195, Cys200, Cys221, and Cys224) were constrained to maintain the tetrahedral coordination geometry during the MD simulation. Nonbonded Lennard-Jones interactions were cut off at 0.9 nm, and long-range electrostatic interactions were handled with the particle-mesh Ewald (PME^{41,42}) method. Periodic boundary conditions were applied throughout the MD simulation.

The rmsd of the backbone atoms was stabilized after a 300 ps simulation. Thus, the average protein structure from a time frame of 350–400 ps was calculated, and further energy-minimization steps with the steepest descent method were performed to create the final SIRT2 protein structure used in the study. Heavy atom rmsd values between the final protein structure and the starting structure of the MD simulation were calculated to ensure that no large-scale structural arrangements have taken place during the MD simulation. In addition, the quality of the final SIRT2 structure was evaluated with the PROCHECK²⁶ program and compared to the original X-ray structure.

Examining the Putative SIRT2 Active Site. After the MD simulation, the putative SIRT2 active site was inspected again for amino acids that were interesting for the virtual screening procedure. The edge of the active site was lined with amino acids Phe96, Tyr104, Pro115, Glu116, Ala186, His187, and Phe235, in addition to amino acids Asp95, Arg97, and Gln167, which were located close to the putative binding site of NAD⁺. Site features included a hydrophobic pocket near the aromatic moieties of phenylalanines 124, 131, and 190, and the hydrophobic parts of leucines 134 and 138. Close to amino acids Ile169 and Asp170 began a narrow channel that extended throughout the entire length of the protein structure. When inspecting the cocrystallized water from the original X-ray structure 1j8f, this channel was filled with water molecules. This suggests the hydrophilic character of this channel. However, there was not any cocrystallized water molecules in the suggested SIRT2 active site, which demonstrates its hydrophobic nature.

The SIRT2 suggested active site was examined using the GRID 20 program²⁸ to determine possible interactions between amino acids of the putative active site and a variety of small functional groups (i.e., probes). Interaction fields were calculated at a resolution of 1.0 Å using the following probes: carbonyl oxygen, phenolic and carboxy hydroxyl group probe (OH), hydrophobic DRY, a methyl group, a tetrahedral cationic NH₂ group (NH₂⁺), and water. The resulting interaction fields were then examined by visualization within the putative SIRT2 active site.

Finally, the inhibitors sirtinol and A3 (Figure 1) were docked at the putative SIRT2 active site with the GOLD docking program version 1.2.⁴³ Docking was carried out to obtain a population of possible conformations and orientations for these inhibitors at the putative active site. These docked conformations were inspected to achieve supportive information for the favorable interaction calculations and for the observations from the putative active site.

Virtual Screening Procedure. On the basis of observations during examination of the putative SIRT2 active site, two different search queries were created for the database search (see the Supporting Information for the graphical representations of the queries). Both queries were receptor-based and contained additional information from the GRID calculations. Features of the queries were selected to give additional flexibility to the search and thus to avoid unnecessary drop outs from the list of potential hit compounds. Lipinski's rule of five⁴⁴ was used in these searches, and its limits were modified to four as the maximum number of hydrogen bond donors and to seven as the maximum number

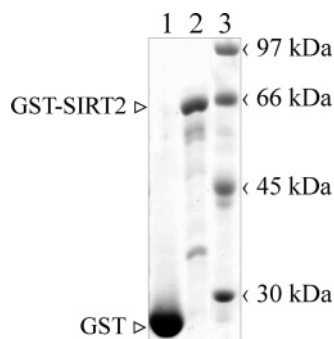


Figure 4. Coomassie stained, SDS-PAGE resolved affinity purified recombinant proteins used in this study: 1, control vector pGEX-2T induced; 2, pTe25 induced; 3, molecular weight markers [low molecular weight calibration kit for SDS electrophoresis (Amersham Biosciences)].

of hydrogen-bond acceptors. Both queries contained either an OH or SH group near amino acids Asp95 and Arg97, with a tolerance of 1.1 Å, and several excluded volumes for outlining the putative active site. Additionally, the first query contained two donor atoms at a tolerance of 1.0 Å, one near amino acids Phe119 and Val233 and the other near His187. Hit compounds were required to contain at least one of these donors. The first query also contained a hydrophobic feature near amino acids Ile169 and Asp170 at a tolerance of 1.3 Å. The second query contained two hydrophobic features at a tolerance of 0.5 Å, one near amino acids Phe119, Phe131, and Phe190 and the other near amino acids Ile169 and Asp170. The purpose of the hydrophobic features in both queries was to select hit compounds having hydrophobic moieties that matched the hydrophobic nature of the putative SIRT2 active site. Database searching was performed as a flexible 3D search in the Maybridge²⁹ database, using the database searching program Unity 4.3.1 implemented in Sybyl.

Database searches resulted in 47 and 24 candidate hit compounds for the first and the second queries, respectively. After removing duplicates, a total of 66 hit compounds remained. The ability of these compounds to permeate the small intestine cells were then predicted with the program VolSurf 3.0^{45,46} implemented in Sybyl. The permeability prediction was introduced as an additional filter of absorption ability. The predictions in the VolSurf model are calculated as an estimation of the ability of the compounds to pass through human intestinal epithelial cells (CaCo-2). This model is based on the correlation between experimentally determined permeability data and molecular descriptors, which are derived from different molecular interaction fields calculated for the compounds of the model. More detailed description of this model is reported by Cruciani et al.⁴⁵ Permeability predictions for the 66 hit compounds were calculated using default settings in Sybyl, along with a grid spacing of 0.5 Å in the calculation of the molecular interaction fields.

After filtering, 44 candidate hit compounds remained. These compounds were docked at the putative SIRT2 active site using the GOLD program. The location of the docked conformations at the active site, as well as their ability to match the requirements of the search queries, was visually evaluated. On the basis of this visual evaluation of the docked conformations in the putative SIRT2 active site, 15 compounds were selected for test their ability to inhibit SIRT2 in vitro.

Recombinant Proteins. Human SIRT2 cDNA, transcript variant 1 as in RefSeq NM012237, was cloned by PCR with the Advantage cDNA Polymerase Mix (BD/Clontech) using sense primer 5'-CCGGATCCATGGCAGAGCCAGAC and antisense primer 5'-CAGAATTCCTGGGGTTTCTCCC. Primers contained recognition sites for *Bam*HI and *Eco*RI restriction endonucleases, respectively (in italics). cDNA synthesized on total RNA from the WI-38 normal human lung fibroblast cell line (ATCC) by M-MLV Reverse Transcriptase (Promega) was used as a template for PCR. The PCR fragment was digested with the appropriate restriction endonucleases and cloned into

the *Bam*HI-*Eco*RI digested pGEX-2T bacterial expression vector (Amersham Biosciences) under the control of a Ptaq inducible promoter. The identity of the resulting plasmid pTe25 insert was verified by sequencing. The *E. coli* strain DH5a [pTe25] culture was induced by 0.2 mM IPTG at 23 °C for 4 h in TB rich medium with vigorous shaking, and the soluble overexpressed recombinant protein was affinity purified on Glutathione Sepharose 4B (Amersham Biosciences) (Figure 4). The identity of the purified proteins was further verified by protein mass spectrometry. The control GST protein preparations did not show any deacetylase activity. The recombinant GST-SIRT2 showed characteristic features attributed to mammalian SIRT2; i.e., its deacetylase activity was dependent on NAD⁺ and could be inhibited by nicotinamide.

Deacetylation Assays. The tubulin peptide MPSDK-TIGG¹⁹ was chemically acetylated with the sodium salt of [³H]-acetic acid (NEN) using a histone deacetylase assay kit (Upstate Biotechnology). The SIRT2 deacetylation reaction was done in 100 μL of 1× HDAC buffer (Upstate Biotechnology) and 500 μM NAD⁺ (Sigma) with 40 000 cpm [³H]peptide and 1 μg recombinant GST-SIRT2 at 37 °C overnight. The released [³H]acetyl was extracted with ethyl acetate and counted by a liquid scintillation counter, according to the histone deacetylase assay kit protocol (Upstate Biotechnology). Each experiment was repeated at least three times.

Acknowledgment. We thank Ulrich Bergmann and Olga Kyrylenko for technical assistance in protein mass spectrometry. James Callaway, Ph.D., is gratefully acknowledged for revising the language. This study was supported by the National Technology Agency of Finland, Academy of Finland, and Finnish Cultural Foundation. P.N. is funded by the Drug Discovery Graduate School (Finland). CSC-Scientific Computing, Ltd. is acknowledged for computational resources.

Supporting Information Available: Structures for the 10 candidate hit compounds that were found to be inactive in vitro, graphical representations for both search queries utilized in the database searching and for the most relevant GRID results. This material is available free of charge via the Internet at <http://pubs.acs.org>.

References

- Khochbin, S.; Verdel, A.; Lemerrier, C.; Seigneurin-Berny, D. Functional significance of histone deacetylase diversity. *Curr. Opin. Genet. Dev.* **2001**, *11*, 162–166.
- Imai, S.; Armstrong, C. M.; Kaerberlein, M.; Guarente, L. Transcriptional silencing and longevity protein Sir2 is an NAD-dependent histone deacetylase. *Nature* **2000**, *403*, 795–800.
- Landry, J.; Sutton, A.; Tafrov, S. T.; Heller, R. C.; Stebbins, J.; et al. The silencing protein SIR2 and its homologues are NAD-dependent protein deacetylases. *Proc. Natl. Acad. Sci. U.S.A.* **2000**, *97*, 5807–5811.
- Chang, J. H.; Kim, H. C.; Hwang, K. Y.; Lee, J. W.; Jackson, S. P.; et al. Structural basis for the NAD-dependent deacetylase mechanism of Sir2. *J. Biol. Chem.* **2002**, *277*, 34489–34498.
- Sauve, A. A.; Schramm, V. L. Sir2 regulation by nicotinamide results from switching between base exchange and deacetylation chemistry. *Biochemistry* **2003**, *42*, 9249–9256.
- Landry, J.; Slama, J. T.; Sternglanz, R. Role of NAD(+) in the deacetylase activity of the SIR2-like proteins. *Biochem. Biophys. Res. Commun.* **2000**, *278*, 685–690.
- Sauve, A. A.; Celic, I.; Avalos, J.; Deng, H.; Boeke, J. D.; et al. Chemistry of gene silencing: The mechanism of NAD⁺-dependent deacetylation reactions. *Biochemistry* **2001**, *40*, 15456–15463.
- Gasser, S. M.; Cockell, M. M. The molecular biology of the SIR proteins. *Gene* **2001**, *279*, 1–16.
- Tanner, K. G.; Landry, J.; Sternglanz, R.; Denu, J. M. Silent information regulator 2 family of NAD-dependent histone/protein deacetylases generates a unique product, 1-O-acetyl-ADP-ribose. *Proc. Natl. Acad. Sci. U.S.A.* **2000**, *97*, 14178–14182.
- Shore, D. The Sir2 protein family: A novel deacetylase for gene silencing and more. *Proc. Natl. Acad. Sci. U.S.A.* **2000**, *97*, 14030–14032.
- Gottschling, D. E. Gene silencing: Two faces of SIR2. *Curr. Biol.* **2000**, *10*, R708–711.

- (12) Lin, S. J.; Defossez, P. A.; Guarente, L. Requirement of NAD and SIR2 for life-span extension by calorie restriction in *Saccharomyces cerevisiae*. *Science* **2000**, *289*, 2126–2128.
- (13) Guarente, L. SIR2 and aging—the exception that proves the rule. *Trends. Genet.* **2001**, *17*, 391–392.
- (14) Guarente, L. Sir2 links chromatin silencing, metabolism, and aging. *Genes Dev.* **2000**, *14*, 1021–1026.
- (15) Hiratsuka, M.; Inoue, T.; Toda, T.; Kimura, N.; Shirayoshi, Y.; et al. Proteomics-based identification of differentially expressed genes in human gliomas: Down-regulation of SIRT2 gene. *Biochem. Biophys. Res. Commun.* **2003**, *309*, 558–566.
- (16) Krämer, O. H.; Göttlicher, M.; Heinzl, T. Histone deacetylase as a therapeutic target. *Trends. Endocrinol. Metab.* **2001**, *12*, 294–300.
- (17) Frye, R. A. Characterization of five human cDNAs with homology to the yeast SIR2 gene: Sir2-like proteins (sirtuins) metabolize NAD and may have protein ADP-ribosyltransferase activity. *Biochem. Biophys. Res. Commun.* **1999**, *260*, 273–279.
- (18) Frye, R. A. Phylogenetic classification of prokaryotic and eukaryotic Sir2-like proteins. *Biochem. Biophys. Res. Commun.* **2000**, *273*, 793–798.
- (19) North, B. J.; Marshall, B. L.; Borra, M. T.; Denu, J. M.; Verdin, E. The human Sir2 ortholog, SIRT2, is an NAD⁺-dependent tubulin deacetylase. *Mol. Cell.* **2003**, *11*, 437–444.
- (20) Dryden, S. C.; Nahhas, F. A.; Nowak, J. E.; Goustin, A. S.; Tainsky, M. A. Role for human SIRT2 NAD-dependent deacetylase activity in control of mitotic exit in the cell cycle. *Mol. Cell. Biol.* **2003**, *23*, 3173–3185.
- (21) Fennin, M. S.; Donigian, J. R.; Pavletich, N. P. Structure of the histone deacetylase SIRT2. *Nat. Struct. Biol.* **2001**, *8*, 621–625.
- (22) Bellamacina, C. R. The nicotinamide dinucleotide binding motif: A comparison of nucleotide binding proteins. *FASEB J.* **1996**, *10*, 1257–1269.
- (23) Bedalov, A.; Gatabonton, T.; Irvine, W. P.; Gottschling, D. E.; Simon, J. A. Identification of a small molecule inhibitor of Sir2p. *Proc. Natl. Acad. Sci. U.S.A.* **2001**, *98*, 15113–15118.
- (24) Grozinger, C. M.; Chao, E. D.; Blackwell, H. E.; Moazed, D.; Schreiber, S. L. Identification of a class of small molecule inhibitors of the sirtuin family of NAD-dependent deacetylases by phenotypic screening. *J. Biol. Chem.* **2001**, *276*, 38837–38843.
- (25) Grozinger, C. M.; Schreiber, S. L. Deacetylase enzymes: Biological functions and the use of small-molecule inhibitors. *Chem. Biol.* **2002**, *9*, 3–16.
- (26) Laskowski, R. A.; MacArthur, M. W.; Moss, D. S.; Thornton, J. M. PROCHECK: A program to check the stereochemical quality of protein structures. *J. Appl. Crystallogr.* **1993**, *26*, 283–291.
- (27) Kleywegt, G. J.; Jones, T. A. Phi/psi-chology: Ramachandran revisited. *Structure* **1996**, *4*, 1395–1400.
- (28) Goodford, P. J. A computational procedure for determining energetically favorable binding sites on biologically important macromolecules. *J. Med. Chem.* **1985**, *28*, 849–857.
- (29) *Maybridge Chemicals Database*; Maybridge Chemicals Co. Ltd.: Trevillet, Tintangel, Cornwall PL34 OHW, England.
- (30) Vaziri, H.; Dessain, S. K.; Ng Eaton, E.; Imai, S. I.; Frye, R. A.; et al. hSIR2 (SIRT1) functions as an NAD-dependent p53 deacetylase. *Cell* **2001**, *107*, 149–159.
- (31) Hempen, B.; Brion, J. P. Reduction of acetylated alpha-tubulin immunoreactivity in neurofibrillary tangle-bearing neurons in Alzheimer's disease. *J. Neuropathol. Exp. Neurol.* **1996**, *55*, 964–972.
- (32) Zhang, Y.; Li, N.; Caron, C.; Matthias, G.; Hess, D.; et al. HDAC-6 interacts with and deacetylates tubulin and microtubules in vivo. *EMBO. J.* **2003**, *22*, 1168–1179.
- (33) *Sybyl 6.8 and 6.8.1*; Tripos Inc.: St. Louis, MO.
- (34) Berman, H. M.; Westbrook, J.; Feng, Z.; Gilliland, G.; Bhat, T. N.; et al. The Protein Data Bank. *Nucleic Acid Res.* **2000**, *28*, 235–242.
- (35) *Quanta 2000 molecular modeling package*; Accelrys Inc.: 200 Wheeler Road South Tower 2nd Floor Burlington, MA 01803-5501.
- (36) Lindahl, E.; Hess, B.; van der Spoel, D. GROMACS 3.0: A package for molecular simulation and trajectory analysis. *J. Mol. Mod.* **2001**, *7*, 306–317.
- (37) van Gunsteren, W. F.; Billeter, S. R.; Eising, A. A.; Hünenberger, P. H.; Krüger, P.; et al. *Biomolecular Simulation: The GROMOS96 manual and user guide*; Hochschulverlag AG an der ETH Zürich: Zürich, Switzerland, 1996.
- (38) van der Spoel, D.; van Buuren, A. R.; Apol, E.; Meulenhoff, P. J.; Tieleman, D. P.; et al. *Gromacs User Manual version 3.0*: Nijenborgh 4, 9747 AG, Groningen, The Netherlands, 2001.
- (39) Berendsen, H. J. C.; Postma, J. P. M.; van Gunsteren, W. F.; Hermans, J. Interaction models for water in relation to protein hydration. *Intermolecular Forces*; D. Reidel Publishing Co.: Dordrecht, 1981; pp 331–342.
- (40) Berendsen, H. J. C.; Postma, J. P. M.; DiNola, A.; Haak, J. R. Molecular dynamics with coupling to an external bath. *J. Chem. Phys.* **1984**, *81*, 3684–3690.
- (41) Darden, T.; York, D.; Pedersen, L. Particle mesh Ewald: An N–log(N) method for Ewald sums in large systems. *J. Chem. Phys.* **1993**, *98*, 10089–10092.
- (42) Essmann, U.; Perera, L.; Berkowitz, M. L.; Darden, T.; Lee, H.; et al. A smooth particle mesh Ewald potential. *J. Chem. Phys.* **1995**, *103*, 8577–8592.
- (43) Jones, G.; Willett, P.; Glen, R. C.; Leach, A. R.; Taylor, R. Development and validation of a genetic algorithm for flexible docking. *J. Mol. Biol.* **1997**, *267*, 727–748.
- (44) Lipinski, C. A.; Lombardo, F.; Dominy, B. W.; Feeney, P. J. Experimental and computational approaches to estimate solubility and permeability in drug discovery and development settings. *Adv. Drug. Delivery Rev.* **1997**, *23*, 4–25.
- (45) Cruciani, G.; Pastor, M.; Guba, W. VolSurf: A new tool for the pharmacokinetic optimization of lead compounds. *Eur. J. Pharm. Sci.* **2000**, *11 Suppl 2*, 29–39.
- (46) Cruciani, G.; Crivori, P.; Carrupt, P.-A.; Testa, B. Molecular fields in quantitative structure-permeation relationships: The VolSurf approach. *J. Mol. Struct. THEOCHEM* **2000**, *503*, 17–30.

JM049933M